

Adaptive phase formation in martensitic transformation

A. G. Khachaturyan, S. M. Shapiro,* and S. Semenovskaya

Department of Mechanics and Materials Science, Rutgers University, P.O. Box 909, Piscataway, New Jersey 08855

(Received 5 December 1990; revised manuscript received 26 March 1991)

It is shown that an appearance of an intermediate martensite phase called adaptive martensite may be expected if the surface energy of a boundary between two orientational variants of the normal martensite phase is very low and the typical lattice-mismatch-related elastic energy is high. The adaptive martensite is formed as an elastically constrained phase when the scale of structure heterogeneities induced by the crystal-strain accommodation is reduced to the microscopic scale commensurate with the twin-plane interplanar distance. An example of the cubic→tetragonal transformation is considered where the adaptive phase has a pseudo-orthorhombic lattice. The crystal-lattice parameters of the adaptive phase are expressed through those of the parent cubic phase and tetragonal normal martensite. It is shown that the $(5\sqrt{2})7R$ martensite in β' NiAl alloys and the intermediate phase recently found just above the temperature of the fcc→fct martensitic transformation in Fe-Pd are examples of the adaptive martensite. A possible role of the adaptive phase in the thermal nucleation of the martensite is discussed. The nucleation of the normal martensite may be bypassed by nucleation of the adaptive phase, which transforms to the normal martensite during the growth.

I. INTRODUCTION

Any structural transformation resulting in reduction of the point symmetry of a crystal lattice produces a crystal-lattice mismatch with the parent phase. The kinetic, structural, and thermodynamic characteristics of the martensitic transformation arise when an elastic energy generated by the crystal-lattice mismatch between the parent and product phases proves to be about equal to or much greater than the transformation chemical driving force, i.e., when $\mu\epsilon_0^2/|\Delta f| \sim 1$ or $\mu\epsilon_0^2/|\Delta f| \gg 1$, where $\mu\epsilon_0^2$ is a typical elastic energy, ϵ_0 is a typical crystal-lattice rearrangement strain characterizing the mismatch between the martensite and parent phases, μ is a typical shear modulus, and Δf is the transformation driving force equal to the difference between the specific free energies of the stress-free product and parent phases. These relations between the transformation-induced elastic energy and the chemical driving force impose severe constraints on the transformation path and make the kinetics and thermodynamics of the “strong” martensitic transformation different from those of the conventional phase transformations. Under these conditions the phase transformation can proceed only along the transformation path providing almost complete accommodation of the crystal-lattice mismatch. The transformation path is characterized by a sequence of mesoscale coherent structures formed by martensitic plates consisting of the quasi-periodic alternation of lamellae of two twin-related orientational variants of the martensitic phase. The habit of these lamellae coincides with the twinning plane (see Fig. 1). According to the geometrical theory by Wechsler, Lieberman, and Read¹ and Bowles and Mackenzie,² the volume ratio of the two variants of the martensite phase should be chosen so that the macroscopic shape change is described by an invariant plane strain, the invariant plane being a habit plane. It has been shown by Khachatu-

ryan³ and Roytburd⁴ that formation of a coherent martensitic plate with this morphology does not generate the volume-dependent elastic energy, which is the only part that could affect the phase equilibrium in classical thermodynamics. The elastic energy proves to be proportional to the habit plane surface and is called (somewhat incorrectly) the energy of the semicoherent interfacial boundary. This elastic energy, together with the conventional surface energy of twin boundaries separating lamellae of two orientational variants, determines the period λ of lamellae (see Fig. 1):

$$\lambda \sim \left[\frac{\gamma_{tw}}{\mu\epsilon_0^2} D \right]^{1/2} = \sqrt{r_0 D} \quad (1)$$

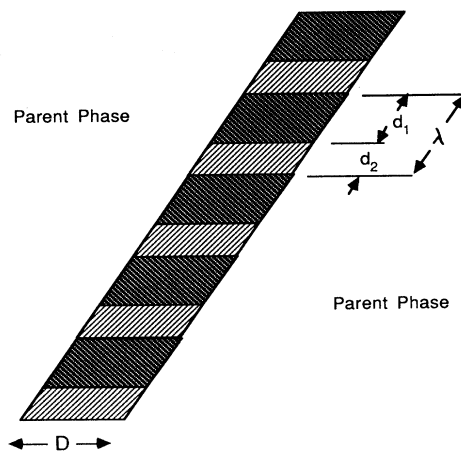


FIG. 1. Schematic representation of the martensitic phase plate composed of twin-related lamellae of two orientation variants of the martensitic phase. The appropriate d_1 -to- d_2 ratio completely accommodates the martensite-to-parent phase macroscopic transformation strain mismatch along the habit plane.

where D is the width of the plate, $r_0 = \gamma_{tw}/\mu\epsilon_0^2$ is a material constant with the dimension of length, γ_{tw} is the twin surface energy, and μ is the shear modulus. If the thickness of the plate, D , is a constant, then the period λ is a constant as well, and the alternation of the twin-related lamellae is periodic. The lamellae in this case can be regarded as elastic domains⁴ because of their profound analogy with the magnetic and ferroelectric domains.⁵ A manifestation of this analogy is the similarity between Eq. (1) and the corresponding equations for the domain size of ferromagnetic and ferroelectric domains.⁶

II. ADAPTIVE MARTENSITE

The martensitic transformation develops through formation of internally twinned plates filling the sample. Like magnetic or ferroelectric domains of large crystals, a typical width of a twinned plate, D , in Eq. (1) is determined by nucleation kinetics, crystal lattice defects, undercooling, and cooling rate.

Let us consider a situation where the typical mesoscale size D and the material constants r_0 are small (small twin surface energy γ_{tw} and large typical elastic energy $\mu\epsilon_0^2$), i.e., where

$$\frac{\gamma_{tw}}{\mu\epsilon_0^2 a_{tw}} < 1$$

(a_{tw} is the atomic interplanar distance for the twinning planes). Then, according to (1), a typical twin size λ also decreases. The decrease can occur only conformally so that the ratio of the volumes of the twin-related lamellae ω is kept constant to maintain the invariant plane transformation strain. This conformal miniaturization of the twinned martensitic structure has a natural crystallographic limitation that the lamellae thickness cannot be less than interplanar distance a_{tw} of the twinning plane and that the thicknesses of twin-related lamellae d_1 and d_2 should be a multiple of this interplanar distance. In other words, the following conditions have to be met:

$$\frac{d_1}{d_2} = \frac{\omega}{1-\omega}, \quad d_1 = m a_{tw}, \quad d_2 = n a_{tw}, \quad d_1 + d_2 = \lambda, \quad (2)$$

where m and n are small integers. Therefore, ω is related to the volume fraction of one variant in the martensite plate shown in Fig. 1. Actually, miniaturization of twins is constrained by a repulsion between the microtwin boundaries. The interaction is substantial when the twin size becomes comparable with the correlation length or, which is the same, with the width of the twin boundary. In the case of sharp boundaries, the minimum thickness of the microtwins is limited by the crystallographic constraint (2).

When lamellae of the twin-related orientational variants reach a size comparable with the interatomic distance a , the mesoscale structure of the martensitic plate becomes a microscale structure. Then the martensite plate has a microtwinned (microinhomogeneous) lattice. This lattice can equally be regarded as an ideal homo-

geneous lattice whose atomic structure is related to the atomic structure of the normal martensite lattice by an appropriate shuffling of crystal planes imitating the twinning plus a certain distortion of these planes and their interplanar distances imitating the homogeneous parent-to-martensite phase transformation strain for the normal martensite. It, of course, should be remembered that the miniaturization may affect the crystal-lattice parameters of the twins when twin width is comparable with the distance between twin boundaries plane. This is actually a twin boundary interaction effect, which is substantial if the distance between the nearest twin boundaries becomes microscopically small.

Hereafter we call this crystal lattice produced by microtwinning (plane shuffling and plane deformation) an adaptive lattice, and we call the corresponding martensite the adaptive martensite. Then the microtwinned martensite plate described above can be regarded as an ideal single-domain crystal coherently imbedded into the parent-phase matrix. The total surface energy of the set of microtwin boundaries is proportional to the martensite phase volume V and is of the order of $\sim(\gamma_{tw}/\lambda)V$. Because of this it should be included in the volume-dependent part of the bulk free energy of the adaptive martensite and thus renormalize the free energy. This raises the specific free energy of the adaptive martensite above the specific free energy of the normal martensite by the value $\sim\gamma_{tw}/\lambda$. The semicoherent elastic energy of the boundary should be included in the interfacial energy between the adaptive martensite and the parent phase. Therefore, the adaptive martensite can be formed only if its renormalized specific free energy is less than the specific free energy of the parent phase (the elastic contribution to the specific free energy of the adaptive martensite vanishes because of the invariant plane strain constraint imposed on the adaptive martensite lattice).

The crystal lattice of the adaptive martensite has lower symmetry than that of the normal (nontwinned) martensite. Particularly, the period λ shown in Fig. 1 becomes a new long period of the adaptive lattice. A fingerprint of the adaptive martensite is the following geometrical property of its crystal lattice: *A unit cell of the adaptive martensite is related to the transformation-related unit cell of the parent phase by an invariant plane strain.*

This necessary condition is a direct consequence of the constrained nature of the adaptive martensite. Its fulfillment can be readily verified for each specific case. The condition imposes a severe geometrical constraint on the crystal-lattice parameters of the adaptive martensite, which is a pure result of the crystal-lattice accommodation. It is very hard to imagine a situation when the values of the crystal-lattice parameters of the stress-free parent phase and homogeneous martensitic phase provide an invariant plane strain crystal-lattice rearrangement by accident.

The second distinguishing feature of an adaptive martensite is that its shuffling planes must always be parallel to the twinning (mirror) plane relating two orientational variants of the normal martensite. For example, this requirement predicts a (110) parent plane for the cubic-to-tetragonal transformation.

The third feature is less obvious. Equation (2) gives

$$\frac{\omega_0}{1-\omega_0} = \frac{m}{n},$$

where the m/n ratio is fixed by the condition that m and n are small integers, whereas ω_0 is fixed by the invariant plane strain requirement and, thus, is unambiguously determined by the crystal-lattice parameters of the crystal lattices of the normal martensite and the parent phase. There is, however, almost no chance that the crystal-lattice parameters are such that the $\omega_0/(1-\omega_0)$ ratio is exactly equal to the simple fraction m/n . The only way to eliminate the mismatch between these two values is to insert faults in the regular alternation, $\cdots d_1 d_2 d_1 d_2 \cdots$, of the microlamellae thicknesses $d_1 = ma_{tw}$ and $d_2 = na_{tw}$. The faults should be the wrong size microlamellae of the normal martensite whose thickness deviates from the regular thicknesses $d_1 = ma_{tw}$ and $d_2 = na_{tw}$ by one or several interplanar distances a_{tw} . The thickness of faults and the distance between them should be tuned up so that the volume ratio of all microtwins belonging to the first orientational variant and microtwins of the second orientational variant (including the faulting twins) is equal to the ratio $\omega_0/(1-\omega_0)$ dictated by the requirement of the variant plane strain for the adaptive martensite. The average distance between "faulted microtwins" together with their thickness determines the position of the diffraction spots generated by the adaptive martensite, which should deviate from the positions determined by the rational period, $\lambda = a_{tw}(m+n)$. This effect is similar to the effect of stacking faults⁷ or correlated faults in a layer structure.⁸ The positions of spots, in general, do not coincide with rational points of the reciprocal lattice. The latter fact, as well as the dependence of the diffraction spot positions on the temperature and composition (through the dependence of ω_0 on the temperature and composition via the crystal-lattice parameters) may create the incorrect impression that the martensite actually is an incommensurate phase. The difference that may distinguish the faulted structure of the adaptive martensite from an incommensurate phase is the dependence of superlattice spot positions of the adaptive martensite on the Brillouin zone. Such a dependence is typical in randomly faulted structures but should not be observed in commensurate structures where the positions of the spots are the same in all Brillouin zones, around different fundamental reciprocal-lattice points.

Finally, a typical feature of the adaptive martensite is sensitivity of its crystal structure to the applied stress. The stress affects the two orientational variants differently, depending on a mutual orientation of their tetragonality axis with respect to the principle axes of the stress tensor. The stress suppresses one variant and promotes the other. As a result, the fraction $\omega_0/(1-\omega_0)$, and, thus, the period λ , change. Large stress can completely eliminate one of the variants and, therefore, transform the adaptive martensite to the normal martensite.

Below we consider a particular, but very important, common case of the cubic-to-tetragonal martensitic

transformation that illustrates the properties of the adaptive martensite. We apply the adaptive martensite concept to the well-investigated cases of Ni-Al and Fe-Pd alloys and compare the calculation and observation results.

III. ADAPTIVE MARTENSITE FOR THE CUBIC-TO-TETRAGONAL CRYSTAL-LATTICE REARRANGEMENT

A cubic-to-tetragonal crystal-lattice rearrangement transforms one of the cubic lattice parameters, a_c , into the parameter c_t of the tetragonal lattice and two other mutually perpendicular parameters, a_c , into the parameter a_t of the tetragonal lattice. Such a transformation generates three orientational variants of the tetragonal phase distinguished by the direction of the tetragonal axis with respect to cubic axes of the cubic parent phase. The tetragonal axis can be parallel to one of the three directions, $[100]_c$, $[010]_c$, and $[001]_c$. The crystal-lattice rearrangements producing these three orientational variants are described by three stress-free strain tensors:

$$\begin{aligned} \epsilon(1)_{ij}^0 &= \begin{pmatrix} \epsilon_{33}^0 & 0 & 0 \\ 0 & \epsilon_{11}^0 & 0 \\ 0 & 0 & \epsilon_{11}^0 \end{pmatrix}, \\ \epsilon(2)_{ij}^0 &= \begin{pmatrix} \epsilon_{11}^0 & 0 & 0 \\ 0 & \epsilon_{33}^0 & 0 \\ 0 & 0 & \epsilon_{11}^0 \end{pmatrix}, \\ \epsilon(3)_{ij}^0 &= \begin{pmatrix} \epsilon_{11}^0 & 0 & 0 \\ 0 & \epsilon_{11}^0 & 0 \\ 0 & 0 & \epsilon_{33}^0 \end{pmatrix}, \end{aligned} \quad (3)$$

where the strain components $\epsilon_{33}^0 = (c_t - a_c)/a_c$, $\epsilon_{11}^0 = (a_t - a_c)/a_c$ describe the crystal-lattice mismatch between the tetragonal phase and the cubic matrix in the stress-free state. The mismatch between any two orientational variants, for example, between the second and the first ones, is, then, described by the difference

$$\begin{aligned} \Delta\epsilon(12)_0 &= \epsilon(1)_{ij}^0 - \epsilon(2)_{ij}^0 \\ &= (\epsilon_{33}^0 - \epsilon_{11}^0) \begin{pmatrix} 1 & 0 & 0 \\ 0 & \bar{1} & 0 \\ 0 & 0 & 0 \end{pmatrix}. \end{aligned} \quad (4)$$

The tensor $\Delta\epsilon(12)_0$ can be rewritten as

$$\begin{aligned} \Delta\epsilon(12)_0 &= \epsilon(1)_{ij}^0 - \epsilon(2)_{ij}^0 \\ &= (\epsilon_{33}^0 - \epsilon_{11}^0)(l_i m_j + l_j m_i), \end{aligned} \quad (5)$$

where $l = (1/\sqrt{2}, \bar{1}/\sqrt{2}, 0)$ and $m = (1/\sqrt{2}, 1/\sqrt{2}, 0)$ are unit vectors along the $[1\bar{1}0]$ and $[110]$ directions of the cubic matrix. Since $\Delta\epsilon(12)_0$ is a symmetrized diadic product, the corresponding stress-free mismatch tensor describes an invariant plane strain. The invariant plane is normal to one of the vectors l or m and thus is either $(1\bar{1}0)_c$ or $(110)_c$. Because of that, *the boundary between the two martensite variants is stress-free if it is parallel to*

either of the two planes, $(1\bar{1}0)_c$ or $(110)_c$. A coherent adjustment of the orientational variants along $(110)_c$ results in their rotation to eliminate the gap on the boundary (see Fig. 2). The rotation angle is

$$\phi = 2 \left[\arctan \frac{c_t}{a_t} - \frac{\pi}{4} \right].$$

It follows from Fig. 2 that two martensite variants are in the (110) twin-related position. Since a martensite crystal is a sandwich composed of alternating twin-related lamellae of two variants of the tetragonal phase, then the total stress-free macroscopic shape change is described by the average of the respective strains

$$\bar{\epsilon}_{ij} = \omega \epsilon(1)_{ij}^0 + (1 - \omega) \epsilon(2)_{ij}^0,$$

where ω and $1 - \omega$ are volume fractions of both orientational variants composing the martensite crystal. To provide a stress-free boundary between the tetragonal phase sandwich and the cubic phase matrix, the mismatch tensor $\bar{\epsilon}_{ij}$ should be an invariant plane strain. This is possible if one of the components of the tensor $\bar{\epsilon}_{ij}$ vanishes. It can vanish only if ϵ_{33}^0 and ϵ_{11}^0 have different signs (i.e., if the martensitic transformation expands one of the cubic axes and contracts two others) and if $|\epsilon_{33}^0| > |\epsilon_{11}^0|$. This is the case for practically all known martensitic transformations. Following the line of reasoning of Refs. 3 and 4 for small strain, we obtain the value $\omega = \omega_0$, providing an invariant plane strain. This value is

$$\omega_0 = \frac{\epsilon_{11}^0}{\epsilon_{11}^0 - \epsilon_{33}^0} > 0. \quad (6)$$

The tensor $\bar{\epsilon}_{ij}$ with ω_0 determined by (6) transforms to

$$\bar{\epsilon}_{ij} = \begin{pmatrix} 0 & 0 & 0 \\ 0 & \epsilon_{33}^0 + \epsilon_{11}^0 & 0 \\ 0 & 0 & \epsilon_{11}^0 \end{pmatrix}. \quad (7)$$

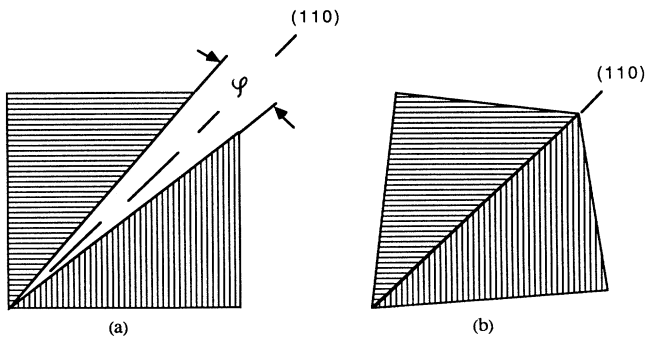


FIG. 2. Rotation due to a coherent adjustment of two orientational variants of the tetragonal normal martensite along the $(110)_c$ plane. Shading indicates the direction of the tetragonal axes distinguishing the variants. (a) A result of the cubic-to-tetragonal transformation described by the strains $\epsilon(1)_{ij}^0$ and $\epsilon(2)_{ij}^0$; (b) the rotation of the angle ϕ to restore a crystal-lattice continuity across the $(110)_c$ boundary plane.

The values ϵ_{11}^0 and $\epsilon_{33}^0 + \epsilon_{11}^0$ have different signs under the current assumption that $|\epsilon_{33}^0| > |\epsilon_{11}^0|$ and ϵ_{33}^0 and ϵ_{11}^0 have different signs. Then the tensor $\bar{\epsilon}_{ij}$ is an invariant plane strain with its habit plane normal to the vector

$$\mathbf{n} = \left[0, \left[\frac{|\epsilon_{33}^0 + \epsilon_{11}^0|}{|\epsilon_{11}^0| + |\epsilon_{33}^0 + \epsilon_{11}^0|} \right]^{1/2}, \left[\frac{|\epsilon_{11}^0|}{|\epsilon_{11}^0| + |\epsilon_{33}^0 + \epsilon_{11}^0|} \right]^{1/2} \right].$$

Although results (6) and (7) are derived in the framework of the linear theory of the martensitic transformation,^{3,4} the vanishing of one of the diagonal components of the average stress-free strain matrix, $\bar{\epsilon}_{11}$, and equality of the other component, $\bar{\epsilon}_{33}$, to ϵ_{11}^0 imposed by an invariant plane constraint are fulfilled for large ϵ_{11}^0 and ϵ_{33}^0 as well.

IV. EXAMPLES OF ADAPTIVE MARTENSITE FOR THE CUBIC-TO-TETRAGONAL TRANSFORMATION

For a small twin-boundary energy γ_{tw} and large typical elastic energy $\mu \epsilon_2^0$ the twin size may reduce and become comparable to the atomic scale size. Then the appearance of the adaptive (microscopically twinned) martensite instead of the normal tetragonal martensite should be expected. If the $(110)_c$ twin-related lamellae of the martensitic phase are microscopically thin, the twinned martensitic plate can be considered as an ideal single crystal of a homogeneous phase, which we regard as adaptive martensite. Let us assume that the macroscopic description of the crystal-lattice rearrangement producing an adaptive martensite lattice is still valid in spite of the microscopic sizes of the twin-related lamellae. Then stress-free strain (7) describes the correspondence between the crystal-lattice parameters of the parent and adaptive martensite lattices. It is clear that the martensitic transformation described by the strain (7) results in the cubic-to-pseudo-orthorhombic crystal-lattice rearrangement. Applying (7) to three cubic axes, $\mathbf{a}_1 = (a_c, 0, 0)$, $\mathbf{a}_2 = (0, a_c, 0)$, and $\mathbf{a}_3 = (0, 0, a_c)$, we can express the crystal-lattice parameters of the adaptive martensite through that of the normal tetragonal martensite c_t , a_t , and of the parent cubic phase a_c :

$$\begin{aligned} a_{ad} &= a_c, \\ b_{ad} &= a_t + c_t - a_c, \\ c_{ad} &= a_t, \end{aligned} \quad (8)$$

where the definitions $a_t = a_c(1 + \epsilon_{11}^0)$, $c_t = a_c(1 + \epsilon_{33}^0)$, and

$$\begin{aligned} b_{ad} &= a_c(1 + \epsilon_{11}^0 + \epsilon_{33}^0) \\ &= a_c(1 + \epsilon_{11}^0) + a_c(1 + \epsilon_{33}^0) - a_c \\ &= a_t + c_t - a_c \end{aligned}$$

are utilized. As has been stated above, the relations (8) between the crystal-lattice parameters of the orthorhombic martensite, the normal martensite, and the parent cubic phase are fingerprints of the adaptive martensite. We should emphasize the following: According to (8), the crystal-lattice parameter of the cubic parent phase a_c and

the parameter of the normal martensite a_t continue into the range of existence of the adaptive martensite becoming its parameters, a_{ad} and c_{ad} . The parameter c_t of the normal martensite is not extrapolated, however, into the adaptive martensite range. The plot c_t versus composition or temperature is terminated at the boundary of the range.

In deriving Eqs. (8) we used an assumption that the crystal-lattice rearrangement of the adaptive martensite can be reasonably well described by the alternating macroscopic strains $\epsilon(1)_{ij}^0$ and $\epsilon(2)_{ij}^0$. This assumption does not affect the equation for a_{ad} and c_{ad} , but it may affect equation for b_{ad} .

Below we compare the observed crystal-lattice parameters of the 7R martensite in β' -Ni-Al alloys and the orthorhombic precursor martensite in Fe-Pd alloys with ones calculated from Eqs. (8) and show that these phases have all the features of the adaptive martensite. This comparison demonstrates that the description of the cubic-phase-to-adaptive-phase crystal-lattice rearrangement by means of the cubic-to-tetragonal transformation strain is in excellent agreement with the available experimental data.

A. Adaptive martensite in β' -Ni-Al alloys

Let us consider, first, the case of the martensitic transformation in the β' -NiAl phase (B2). The cubic-to-tetragonal transformation of this phase is characterized by the Bain distortion transforming the CsCl-type cubic structure of the β' -NiAl phase to the $L1_0$ (CuAuI-type) tetragonal structure (Fig. 3), which we shall regard as a normal martensite. The normal martensite has been observed in this system by Enami *et al.*⁹ who have shown that β' -NiAl alloys containing 62–64 at. % Ni really have a $L1_0$ structure. There are indications that the stacking fault energy of the alloys is very low, since the observed $L1_0$ martensite contains a large quantity of $(111)_{L1_0}$ stacking faults and thin twins.^{10–12}

Since the $(111)_t$ plane of the $L1_0$ phase is actually formed by the Bain distortion from the $(110)_c$ plane of the

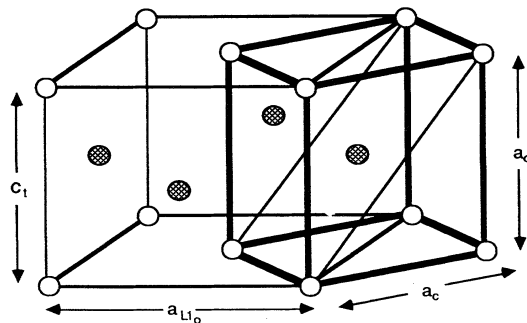


FIG. 3. Bain B2 (CsCl-type cubic lattice) \rightarrow $L1_0$ (tetragonal CuAuI-type) crystal-lattice rearrangement producing the normal martensite in β' -NiAl alloys. The bold lines delineate the cubic structure. Ni and Al atoms are shown by different circles. The $(110)_{B2}$ plane, shown by thin lines, transforms to the $(111)_{L1_0}$ plane after the B2 \rightarrow $L1_0$ martensitic transformation.

the B2 structure, the appearance of many $(111)_{L1_0}$ twins and stacking faults actually means that the surface energy of the $(110)_c$ twins is very low, and, thus, the appearance of the adaptive martensite in these alloys can be expected.

Shapiro *et al.* reported that the crystal lattice parameter of the parent B2 cubic phase matrix of the A1–62.5 at. % Ni alloy is $a_c = 2.857 \text{ \AA}$.¹³ Martynov *et al.*^{14,15} reported the crystal-lattice parameters of the tetragonal $L1_0$ martensite with 63.1 at. % Ni:

$$a_t = \frac{1}{\sqrt{2}} a_{L1_0} = \frac{3.83}{\sqrt{2}} = 2.708 \text{ \AA}, \quad c_t = c_{L1_0} = 3.18 \text{ \AA}.$$

Using these data and $a_c = 2.857 \text{ \AA}$ reported in Ref. 13, we can calculate the mismatch tensor components ϵ_{11}^0 and ϵ_{33}^0 . Calculating the crystal-lattice parameters of the adaptive martensite using the measured data for the crystal-lattice parameters of the matrix phase and normal $L1_0$ martensite by means of Eq. (8) gives

$$a_{ad} = a_c = 2.857 \text{ \AA},$$

$$b_{ad} = a_t + c_t - a_c = 2.708 + 3.18 - 2.857 = 3.031 \text{ \AA},$$

$$c_{ad} = a_t = 2.708 \text{ \AA},$$

which, as it follows from Fig. 4, are in an excellent agreement with the measured values for the pseudo-orthorhombic unit cell of the 7R martensite:¹³

$$a_{7R} = 2.845 \text{ \AA}, \quad b_{7R} = 3.022 \text{ \AA}, \quad c_{7R} = 2.709 \text{ \AA}.$$

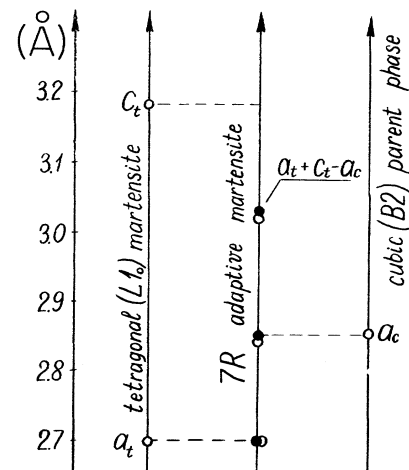


FIG. 4. Relation between observed crystal-lattice parameters of NiAl, c_t and a_t , of the normal tetragonal $L1_0$ martensite (left axis, open circles), observed lattice parameters of the pseudo-orthorhombic 7R martensite (medium axis, open circles), the cubic B2 parent phase, a_c (right axis, open circles), and the parameters of the adaptive martensite calculated according to Eq. (8) (medium axis, solid circles). The dashed line emphasizes equality, $a_{ad} = a_c$ and $c_{ad} = a_t$. This figure illustrates an excellent agreement with the prediction (8) showing that the 7R martensite is an adaptive phase.

Therefore the main criterion, fulfillment of Eq. (8), which allows us to interpret the 7R phase as the adaptive martensite, is met. The agreement between the calculated parameter b_{ad} and the observed one b_{7R} confirms that the macroscopic description of the microtwinning by means of the homogeneous $B2 \rightarrow L1_0$ Bain distortion is still accurate in spite of the microscopic sizes of the twin components with thicknesses $d_1 = 2a_{tw}$ and $d_2 = 5a_{tw}$. The agreement is sufficiently conclusive, since the calculation results are very sensitive to the input crystal-lattice parameters of the $B2$ and $L1_0$ phases. It should also be mentioned that actually the adaptive martensite should be slightly monoclinic because of the rotation of the microtwins shown in Fig. 2.

Now we check whether the 2/5 ratio of twin-related layers forming the 7R structure is the same value as the $\omega_0/(1-\omega_0)$ ratio of the thicknesses of the orientational variants, which is predicted for the adaptive martensite. The $\omega_0/(1-\omega_0)$ ratio is expressed through the crystal-lattice parameters of the $B2$ and $L1_0$ phases by Eq. (6). With $a_c = a_{B2} = 2.857 \text{ \AA}$,¹³ and $a_t = (1/\sqrt{2})a_{L1_0} = 2.708 \text{ \AA}$, $c_t = c_{L1_0} = 3.18 \text{ \AA}$,¹⁴ equations $\epsilon_{33}^0 = (c_t - a_c)/a_c$ and $\epsilon_{11}^0 = (a_t - a_c)/a_c$ give $\epsilon_{33}^0 = 0.113$ and $\epsilon_{11}^0 = -0.052$. Using these strain components in Eq. (6) gives the value, ω_0 , of the volume fraction of the variant of the $L1_0$ normal martensite generated by the transformation strain $\epsilon(1)_{ij}^0$:

$$\omega_0 = \frac{\epsilon_{11}^0}{\epsilon_{11}^0 - \epsilon_{33}^0} = 0.31 .$$

If, however, the same strain components are calculated from the observed parameters for the 7R (Ref. 13) using Eq. (8), then Eq. (6) gives $\omega_0 = 0.30$. The microscopic structure of the microtwinning adaptive martensite with the smallest possible period, λ , and the d_1/λ ratio closest to $\omega_0 \approx 0.3$ is provided by the $d_1/d_2 = 2/5$ ratio, which corresponds to the value $\omega_0 = d_1/\lambda = 2/(2+5) \approx 0.29$. This demonstrates that the ratio $\omega_0 = 0.31$ calculated from the crystal-lattice parameters of the parent and normal martensite phases proves to be very close to the 2/7 ratio and, thus, leads to the formation of an adaptive phase with the 7R structure.

The atomic structure generated by alternation of the microtwins with thicknesses, $d_1 = 2a_{tw}$ and $d_2 = 5a_{tw}$ can be readily constructed. Using the standard A, B, C designations for the positions of the close-packed $(111)_{L1_0}$ planes and taking into account that the $L1_0$ structure is formed by the $\cdots ABCABCABC \cdots$ sequence of the close packed planes, we obtained the following sequence for the adaptive microtwinning martensite:

$$\cdots ABCABA^-C^- ABCABA^-C^- ABCABA^-C^- \cdots ,$$

where the period λ represents $ABCABA^-C^-$ and the minus sign means the shear of the opposite direction. The corresponding structure is shown in Fig. 5. This is just the structure reported for the 7R ($5\sqrt{2}$) phase.

The mismatch between these two values, $\omega_0 \approx 0.30$ and ≈ 0.29 , can be, for example, accommodated by faulting

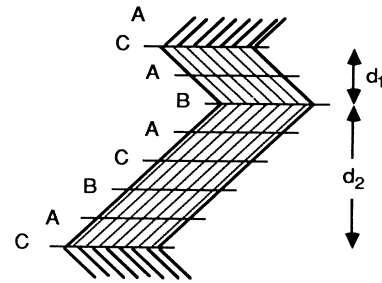


FIG. 5. Microtwins in the 7R martensite in a NiAl alloy. The atomic structure is described by the $ABCABA^-C^-$ sequence of the close packed (111) planes in the $L1_0$ structure; d_1 and d_2 are widths of the twin-related variants of the “tetragonal” microscopic layers. This microtwin structure can be also regarded as an ideal long-period structure.

the periodic 7R sequence (substituting microtwins with the thickness $d'_1 = 3a_{tw}$ for the regular microtwins with the thickness $d_1 = 2a_{tw}$ makes the average distance between faults equal to $\sim 8\lambda = 56a_{tw}$). Then the total volume fraction of the microtwins increases from the value ~ 0.29 determined by the $(\sqrt{2}, 5)$ 7R structure to the value ~ 0.30 dictated by the invariant plane requirement. The random faulting would result in a shift of the superlattice spots of the 7R structure from their ideal positions corresponding to the rational period $\lambda = 7a_{tw}$, the shift being different in different Brillouin zones. This effect was observed by Shapiro *et al.*¹³ who first recognized that such an irregular shift rules out the interpretation of the 7R structure as an incommensurate periodic structure.

Another distinguishing feature that indicates that the 7R phase is actually an adaptive martensite is its response to the applied stress. As discussed above, if the 7R martensite is an adaptive phase, its periodicity and relation between thicknesses of microtwins, d_1/d_2 , should be very sensitive to the applied stress. Thus, the position of the superlattice spots should be sensitive too. Particularly, if the direction of the applied stress promotes one of the orientational variants suppressing the other, then the second variant disappears, and, thus, the $L1_0$ normal tetragonal phase emerges. This prediction seems to be confirmed by Martynov and co-workers^{14,15} who reported the appearance of the $L1_0$ martensite instead of the 7R martensite under applied stress.

It should be emphasized that the formation of the adaptive phase by microtwinning of the $L1_0$ tetragonal phase, which is discussed here, and the conventional shuffling mechanism supplemented by elastic distortion produce the same end result, the 7R structure of NiAl.

As has been shown above, the crystal-lattice parameters of the normal $L1_0$ martensite and the bcc parent phase in Ni-Al alloys provide an invariant plane strain if the volume fraction of microtwins, ω_0 , is close to the $2/(2+5)$ ratio. The atomic structure with such a ratio is generated by a periodical repetition of “microtwins” whose thickness is two $(111)_{L1_0}$ interplanar layers. If, however, the crystal-lattice parameters of the normal

martensite and parent phases are different from those of NiAl, it is possible that an invariant plane strain may be provided by microtwins whose thickness is one $(111)_{L1_0}$ layer. Such microtwins are actually stacking faults in the $ABCABC$ sequence of the $(111)_{L1_0}$ planes generating the normal $L1_0$ martensite. For example, if ω_0 is close to the $1/3$ ratio, the resultant "microtwinned" structure of the adaptive martensite is generated by the $A^-BCB^-CAC^-AB$ sequence of the $(111)_{L1_0}$ planes. A martensite with this structure is called a $9R$ martensite. If ω_0 deviates from a simple ratio, such as $1/3$, faults in the regular $9R$ sequence should be introduced to accommodate the deviation. If faults are random, it results in the displacement of the diffraction maxima, which are different in different Brillouin zones. This situation is not unusual for systems with layer faulting. The best-known example is a shift of diffraction maxima in the fcc lattice caused by stacking faults (see, for instance, Ref. 16). Faulting caused by stacking faults, which we regarded above as one-layer microtwins, was also determined to be the origin of unusual shifts of Bragg peaks in $9R$ phase in Na and Li.¹⁷ The shift of the diffraction maxima, different in different Brillouin zones, has been, for example, observed by Noda *et al.* in the $9R$ martensite in Ni-Ti(Fe) alloys.¹⁸

An important and nontrivial conclusion that the crystal structure of many long-period martensites in nonferrous β phase alloys is determined by an accommodation of the martensite lattice to the parent phase lattice actually has been made in earlier works. These works are, particularly, summarized and discussed in the review paper by Warlimont and Delaey.¹⁹ In these works the structure of the long-period martensite has been derived from the condition of the stacking-fault-induced accommodation transforming the Bain strain to an invariant plane strain. Therefore, these martensite phases are actually also adaptive phases in the sense discussed above. Their structure can also be derived from the twin-related variants of the normal martensite phase by their conformal miniaturization to the microscopic sizes in exactly the same way as the structure of the $7R$ martensite. The long-period structures appear when the width of thinner microtwins is reduced to that of the interplanar layer.

The long-period martensite formation is expected if the lattices of the normal tetragonal martensite and cubic parent matrix accommodate under condition $\gamma_{tw}/\mu\epsilon_0^2 a_{tw} < 1$, i.e., when the surface energy of the $(110)_c$ twin is very low and the $L1_0/B2$ crystal-lattice mismatch is large. If, however, $\gamma_{tw}/\mu\epsilon_0^2 a_{tw} \ll 1$, which is probably the case for a martensite in the β phase alloys, this martensite does not transform to the normal martensite upon the cooling but may exist in the thermoelastic equilibrium at all temperatures.

B. Adaptive martensite in Fe-Pd

Fe-30.1 at. % Pd alloys undergo the fcc \rightarrow fct martensitic transformation as shown by Matsui, Yamada, and Adachi²⁰ and M. Sugiyama, Ohshima, and Fujita.²¹ Seto, Noda, and Yamada²² discovered an intermediate phase

within the narrow range between 265 and 273 °K above the fcc \rightarrow fct transformation temperature. The crystal-lattice parameters of this phase were measured by these authors using a high-resolution x-ray single-crystal technique. These observations suggest that the observed intermediate phase is the adaptive martensite. Whether this is so can be established if the characteristic features of the adaptive martensite, extensively discussed above, were found in this intermediate phase. Particularly, the intermediate phase can be attributed to the adaptive martensite if the crystal-lattice parameters of the adaptive martensite, a_{ad}, b_{ad}, c_{ad} , calculated from the crystal-lattice parameters of the cubic parent phase and the normal martensite by using Eq. (8) are equal (or very close) to the observed parameters of the intermediate phase.

The dependence of the crystal-lattice parameters of the fcc phase, normal fct martensite, and the intermediate phase on the temperature measured by Seto, Noda, and Yamada²² is presented in Fig. 6. It follows from Fig. 6 that in accordance with the theoretical predictions for the adaptive martensite, the parameters a_c and a_t continue into the intermediate phase range becoming its parameters, a_{ad} and c_{ad} , respectively. This observation is consistent with the first and the third equations in (8). The observed parameter c_t , also in accordance with the predictions, is abruptly terminated at the boundary tempera-

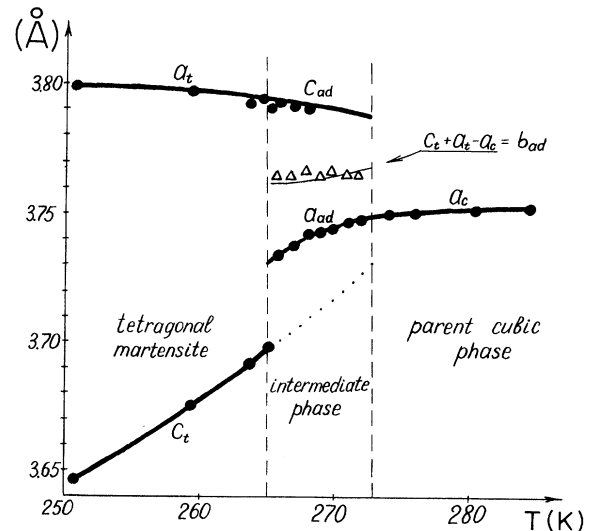


FIG. 6. Fe-30.1 at. % Pd. Observed crystal-lattice parameters of the tetragonal fct martensite (a_t, c_t), cubic fcc parent phase (a_c), and the intermediate phase (Ref. 22). The temperature dependences of a_t , c_t , and a_c are shown by bold lines. The dashed vertical lines indicate the stability range of the intermediate phase, which is actually the adaptive martensite. The experimental data illustrates that the parameters a_t and a_c of the normal martensite and parent phase are continued into the adaptive martensite field becoming, in accordance with prediction (8), the parameters c_{ad} and a_{ad} , respectively. The parameter c_t , vs the T plot, is terminated at the intermediate phase boundary. Dots shown are the extrapolation to calculate the third parameter of the intermediate phase, $b_{ad} = a_t + c_t - a_c$. Triangles indicate the experimental points for b_{ad} .

ture between the tetragonal and intermediate phase. The parameter $b_{ad} = a_t + c_t - a_c$ calculated for the adaptive martensite from parameters a_t, c_t, a_c extrapolated into the intermediate phase range is shown by a thin line. Figure 6 shows the excellent agreement between this calculated line for the adaptive martensite and the experimental points for the intermediate phase. This agreement is so good that we believe it proves that the intermediate phase is actually the adaptive martensite, which is actually a microtwinned fct phase.

We can estimate the twin volume fraction, ω_0 , providing the invariant plane transformation strain for the adaptive phase using the observed crystal-lattice parameters, taken from Fig. 6, $c_t = 3.697 \text{ \AA}$, $a_t = 3.792 \text{ \AA}$, $a_c = 3.730 \text{ \AA}$, at $T \approx 266 \text{ K}$ and $c_t = 3.730 \text{ \AA}$, $a_t = 3.787 \text{ \AA}$, $a_c = 3.750 \text{ \AA}$, at $T \approx 273 \text{ K}$. Substituting these values into equations

$$\epsilon_{11}^0 = \frac{a_t - a_c}{a_c} \quad \text{and} \quad \epsilon_{33}^0 = \frac{c_t - a_c}{a_c}$$

gives the transformation strain components. The volume fraction, ω_0 , corresponding to the observed crystal-lattice parameters, can then be determined by substituting the numerical values of ϵ_{11}^0 and ϵ_{33}^0 into Eq. (6). The calculation gives $\omega_0 = 0.652$ at $T = 265 \text{ K}$ and $\omega_0 = 0.649$ at $T = 273 \text{ K}$. These volume fractions are slightly below $\omega_0 = \frac{2}{3}$, which corresponds to the 2:1 ratio of the microtwin components.

The displacive transformation in the Fe-30.1 at. % Pd alloy seems to be a second-order transition where a typical tetragonal distortion, $\epsilon_0 = \epsilon_{11}^0 - \epsilon_{33}^0$, plays the part of a long-range order parameter. If we assume that the intermediate phase in Fe-Pd alloys is the adaptive martensite, we can predict the following characteristics of this martensite.

(1) The intermediate phase composed of the periodic alternating microtwins with the microscopic thicknesses, $d_1 = ma_{tw}$ and $d_2 = na_{tw}$, is actually a long-period structure with period $\lambda = (m+n)a_{tw}$. The smaller the period λ of the microtwin structure, the smaller is the elastic strain energy.⁵ The estimated d_1/d_2 ratio, from the condition of an invariant plane strain, is close to 2:1. The maximum possible miniaturization of the microtwin structure consistent with the 2:1 ratio occurs when the adaptive phase is a periodic layer structure with $\lambda = 3a_{tw}$. This structure is described by the $AABAB$ sequence, where A and B designate twin-related atomic layers whose width is the interplanar distance of the (110) twinning plane, a_{tw} . Tripling the periodicity of the (110) layer structure in the fcc lattice should generate the superlattice diffraction spots of the $\frac{2}{3}(110)$ generic type. The intensity of the superlattice spots should be very low, since it is proportional to the squared long-range order parameter, $\epsilon_{11}^0 - \epsilon_{33}^0$, which is small near the second-order transition.

It should, however, be remembered that the $\frac{2}{3}(110)$ structure discussed above is actually the limiting case of a structure with a minimum period consistent with the $\omega_0 \approx \frac{2}{3}$ constraint imposed by the elastic energy accommodation. This structure is predicted under the

assumption that the correlation length (the width of the twin boundary) is less than, but nearly equal to, the width of one interplanar layer a_{tw} . Otherwise, the adaptive structure has to multiply its parameters conformally in accordance with the increasing correlation length; i.e., the period may be described by one of the following periodic sequences whose translational motifs are $AAAABB$ (doubling), $AAAAABBB$ (tripling), etc. All these motifs maintain their 2:1 microtwin A/B ratio. In these cases, however, the faulting mechanism can be even more complex.

(2) As has been mentioned above, the complete elastic accommodation occurs at the calculated value ω_0 , which deviates slightly from the nearest rational fraction $m/(m+n) = \frac{2}{3}$ associated with the regular $\cdots AABAB \cdots$ sequence. This deviation is compensated by the appearance of "faulted twins" in the regular sequence such as



where underlined faults have an extra B layer. This faulted sequence reduces ω_0 from the value $\frac{2}{3}$ approaching the values 0.652 and 0.649 calculated for different temperatures. The average distance between faults determines the deviation of ω_0 from $\frac{2}{3}$. The longer the distance, the smaller the deviation is. One can readily see that the value ω_0 is related to average separation distance between faults by the relation

$$\omega_0 = \frac{2\bar{n}}{3\bar{n} + 1}, \quad (9)$$

where $\bar{n} - 1$ is the average number of the AAB elements of the regular sequence between the nearest faults, and $3(\bar{n} - 1)a_{tw}$ is an average separation distance between the faults.

The intermediate phase structure should be very sensitive to the alloy temperature, since the crystal-lattice parameters a_t, c_t, a_c , determining the volume fractions of microtwins, ω_0 and $1 - \omega_0$, are strongly dependent on the temperature. This dependence should result in the temperature dependence of the thicknesses of the microtwins d_1, d_2 and, thus, should affect the period λ and the average distance between faulted microtwins.

It follows from Eq. (9) that the temperature dependence of ω_0 , varying from 0.652 to 0.649 gives the variation of \bar{n} from 15 to 12. This means that the calculated values of ω_0 providing the complete accommodation of the volume-dependent elastic energy can be obtained by faulting if the average separation distance between faults, $3(\bar{n} - 1)a_{tw}$, is between $42a_{tw}$ and $33a_{tw}$. If faults were random, the diffraction pattern generated by the faulted microtwins would have an appearance of a pattern generated by an incommensurate phase, but unlike the real periodic incommensurate phase, the superlattice diffraction spots generated by the alternating microtwins with faults would be dependent on the Brillouin zone. This phenomenon should be similar to that observed in Ref. 13 and 18 for Ni-Al and Ni-Ti(Fe) alloys.

(3) If faults are distributed periodically, which would minimize the elastic energy, then the adaptive phase is a commensurate long-period structure whose period λ is determined by the distance between faults:

$$\lambda = a_{\text{tw}}(3n + 1),$$

where n is an integer between 15 and 12. Then the temperature and concentration variations of the crystal-lattice parameters of the parent fcc phase and normal martensite should result in the appearance of the homologous series of the adaptive phases whose crystallographic motif can be presented as $(AABB)(AAB)^{n-1} = A^{2n}B^{n+1}$.

(4) The range of the intermediate phase and its structure should be very sensitive to the applied stress. Using the conventional Landau expansion for the free energy near the second-order transition point with respect to the long-range order parameter (which is proportional to the tetragonal distortion ϵ_0) to calculate the twin-boundary energy γ_{tw} , one can readily show that the ratio $\gamma_{\text{tw}}/\mu\epsilon_0^2$ vanishes when the temperature approaches the second-order transition temperature. As has been mentioned above, the adaptive phase is expected if the $\gamma_{\text{tw}}/(\mu\epsilon_0^2 a_{\text{tw}})$ ratio is small. Therefore the formation of the adaptive phase can be expected just below the second-order transition. The corresponding miniaturization of microtwins in this case is limited. The twin width cannot be much smaller than the correlation length determining a typical radius of interaction between nearest twin boundaries. A decrease of the temperature would result in an increase of the $\gamma_{\text{tw}}/\mu\epsilon_0^2$ ratio and, thus, the transition from the adaptive to the normal martensite. These conclusions seem to agree with the observation of the adaptive phase in Fe-30.1 at. % Pd within the narrow temperature range (about 8°) below the temperature ~ 273 K and its transformation to the normal martensite below approximately 265 K.

V. A POSSIBLE ROLE OF THE ADAPTIVE PHASE IN THE THERMAL NUCLEATION OF A MARTENSITE

As is known, the strong martensitic transformation with a large crystal-lattice mismatch ($\mu\epsilon_0^2/|\Delta f| \gg 1$), such as the fcc \rightarrow bcc or bcc \rightarrow fcc transformations, cannot homogeneously nucleate, since the elastic energy generated by a coherent homogeneous nucleus of the martensitic phase is too high. Actually, this elastic energy barrier completely blocks the nucleation via thermal fluctuations at any undercooling. However, the transformation path through the nucleation of homogeneous particles of the normal martensitic phase is not the only option. The transformation may bypass such a nucleation and, instead of homogeneous particles of the normal martensite, particles of the adaptive phase may nucleate. The adaptive phase nucleation does not generate the volume-dependent elastic energy and, thus, is not blocked by the elastic strain barriers. From the crystallographic and thermodynamic viewpoint the adaptive phase may be regarded as just a conventional metastable phase whose free energy is slightly higher than that of the stable normal martensite but whose nucleation, unlike the nucleation of the normal martensite, does not substantially raise the

elastic energy. Thus, the nucleation of the homogeneous adaptive martensite particles can occur conventionally in the same way as the classical nucleation of a phase with a low crystal-lattice mismatch. The growth of the adaptive phase nuclei should, according to Eq. (1), increase the equilibrium microtwin sizes $d_1 = \omega_0 \lambda$ and $d_2 = (1 - \omega_0) \lambda$ up to the stages where they reach the macroscopic scale. Then the resultant structure is actually a conventional structure of the normal macroscopically twinned martensite. Observation of the adaptive martensite is possible only if the coarsening of the microtwins is hindered either by the low surface energy of the twins, γ_{tw} , or for other reasons. It is possible that so-called premartensitic phenomena observed above the temperature of the martensitic transformation M_s in some of the martensitic transformations are caused by fluctuational formation of nuclei of the adaptive martensite or by their formation on crystal-lattice defects.

The appearance of the transient adaptive phase is thermodynamically possible only below the temperature T_{ad} of the congruent stress-free equilibrium between the parent phase and the adaptive martensite. This temperature is, of course, lower than the temperature T_0 of the congruent stress-free equilibrium between the parent phase and the more stable normal martensite. It is possible that the undercooling required to start the martensitic transformation is partially associated with this fact.

Since the formation of the adaptive martensite, by its definition, does not generate a volume-dependent contribution to the free energy, the volume-dependent change of the free energy consists of two terms only, the "chemical" free-energy change in the stress-free state and the positive free-energy contribution associated with the microtwins. They are the first and second terms in the equation

$$\Delta F_{\text{bulk}} = [\Delta f(T)_{\text{chem}} + 2\gamma_{\text{tw}}/\lambda]V,$$

where V is a transformed volume, $\Delta f(T)_{\text{chem}}$ is the change of the specific free energy at the stress-free parent phase-to-normal martensite phase transformation at temperature T . The parent-to-normal martensite phase congruent equilibrium temperature T_0 is, by definition, determined by the equality $\Delta f(T_0)_{\text{chem}} = 0$. The temperature of the congruent stress-free equilibrium between the adaptive martensite and parent phase, T_{ad} , is determined by a similar equation,

$$[\Delta f(T_{\text{ad}})_{\text{chem}} + 2\gamma_{\text{tw}}/\lambda] = 0.$$

The reduction of the transformation temperature due to the microtwin surface energy positive contribution is determined by the Clausius-Claperon equation,

$$\frac{T_0 - T_{\text{ad}}}{T_0} \approx \frac{2\gamma_{\text{tw}}}{Q\lambda}, \quad (10)$$

where Q is the heat effect at the parent-to-normal martensite phase transformation. If γ_{tw} is very low, then both temperatures, T_0 and T_{ad} , are close. If γ_{tw} is large, then the undercooling required to get the adaptive martensite is also large, in which case we can expect a large

temperature hysteresis between the equilibrium temperature T_0 and the M_s temperature.

Let us roughly estimate the difference $\Delta T = T_0 - T_{ad}$ for the Fe-30 at. % Ni alloy with the fcc \rightarrow bcc martensitic transformation. Although nobody observed the adaptive phase in this system, the phase may be important as a transient state required to bypass the strain-induced nucleation barrier. Let us assume that the microtwins producing the adaptive phase are a result of the miniaturization of the conventional $(110)_{fcc}$ twins in this system. The $(110)_{fcc}$ twins in the fcc parent lattice become $(112)_{bcc}$ twins in the martensite bcc lattice. The surface energy $\gamma_{tw} \sim 10$ erg/cm² of the $(112)_{bcc}$ accommodation twins has been estimated for this system in Ref. 5 using, in Eq. (1), the twin size λ and martensite plate thickness D , observed by Maki and Wayman.²³ The heat effect, $Q = 1.218 \times 10^{12}$ erg/mol = 1.73×10^0 erg/cm³ was reported in.²⁴ The calculated value ω_0 for this system is close to 0.4. Actually, we do not know the degree of the miniaturization of microtwins in Fe-Ni alloys, but let us, for microtwins, assume the smallest possible width for, d_1 and d_2 . Then the widths of the twin-related layers consistent with $\omega_0 = 0.4$ are $d_1 = 2a_{tw}$ and $d_2 = 3a_{tw}$, where $a_{tw} = d_{(112)}$ is an interplanar distance of the twinning $(112)_{bcc}$ plane. Therefore, $\lambda = d_1 + d_2 = 5a_{tw} = 5a_{bcc}/\sqrt{6}$, where $a_{bcc} = 2.86$ Å. Using the above numerical values in

(10) gives

$$\frac{T_0 - T_{ad}}{T_0} \sim 0.2.$$

In the relevant situation of the comparatively large twin surface energy, γ_{tw} , the adaptive transient martensite formed during nucleation should immediately transform to the normal martensite in the growth process. The above-estimated 20% undercooling of the Fe-30 at. % Ni alloy, required to start the thermal nucleation of the adaptive martensite and its immediate transformation to the normal bcc martensite, is a very substantial value. It may be partially responsible for the large undercooling with respect to the temperature of the stress-free fcc \rightarrow bcc congruent equilibrium required to start the martensitic transformation.

To accommodate the bulk elastic energy completely, the nuclei of the adaptive martensite should be platelets whose habit plane is parallel to the invariant plane.^{3,5} Part of the remaining elastic energy is proportional to the habit plane surface and, thus, can be included in the parent/martensite phase surface energy. The other remaining part of the elastic free energy is proportional the platelet perimeter. It is described by the same equation as the energy of a dislocation loop with the efficient Burgers vector,⁵

$$\mathbf{b} = (\epsilon_{33}^0 - \epsilon_{11}^0) \left[0, \left[\frac{|\epsilon_{33}^0 + \epsilon_{11}^0|}{|\epsilon_{11}^0 + |\epsilon_{33}^0 + \epsilon_{11}^0|} \right]^{1/2}, \left[\frac{|\epsilon_{11}^0|}{|\epsilon_{11}^0 + |\epsilon_{33}^0 + \epsilon_{11}^0|} \right]^{1/2} \right]. \quad (11)$$

This analogy with a dislocation loop is not accidental, since a platelet characterized by an invariant plane strain generates the same elastic strain field as a conventional dislocation loop in the invariant plane with the above Burgers vector. Therefore, any segment of normal dislocations (they are always present in the parent phase matrix) whose Burgers vector has a direction close to \mathbf{b} in Eq. (11) should facilitate formation of the adaptive martensite nuclei and, thus, serve as a nucleation site.

VI. DISCUSSION

As shown above, the adaptive phase is a metastable alternative to the normal martensitic phase. The adaptive phase cannot exist in the stress-free unconstrained state. It forms only in a constrained state when formation of a more stable normal martensite is suppressed by a large transformation-induced elastic energy. A crystal lattice of the adaptive phase is geometrically derived from that of the normal martensite phase by crystal-plane shuffling, which can be regarded as a microscopic limit of conventional accommodation twinning with twin thicknesses of one or several atomic layers. The main geometrical feature of the crystal lattice of the adaptive phase is that it is related to the parent phase lattice by an invariant

plane crystal-lattice rearrangement. Only then will the volume-dependent part of the elastic energy vanish (it is the only cause of the adaptive phase formation).

Also, the concept of an adaptive phase may be important in resolving the problem of the thermal nucleation of the martensite. As is known, the formation of a critical nucleus of a conventional martensite increases the elastic energy and, thus, increases the nucleation barrier to such an extent that the barrier cannot be surmounted by thermal fluctuations. This completely blocks the thermal nucleation, but the system may bypass this barrier by nucleating the metastable adaptive phase instead of the final martensite phase. The nuclei of the adaptive phase may later easily transform to the normal martensite during the growth stage when the coarsening increases the nucleus size D to the values where the twin width $\omega_0\lambda$, related to D by Eq. (1), reaches macroscopic size. Then the coarsening kinetics, unlike nucleation, do not require overcoming the volume-dependent elastic barriers. Therefore, the martensitic transformation through a transient adaptive phase is a mechanism that may explain the thermofluctuative homogeneous nucleation during a strong martensitic transformation, unassisted by "built in" crystal-lattice defects.

The smaller the twin surface energy and the greater the

crystal-lattice mismatch, the easier it is to form an adaptive martensite. Depending upon these factors, different cases can be expected: (i) a sufficiently stable adaptive martensite existing over a wide or even entire temperature range such as in the cases of the $7R$ martensite and similar long-period martensites in nonferrous β phase alloys (very low γ_{tw}), (ii) the intermediate case when the adaptive martensite exists only within a narrow temperature range above the temperature of the martensitic transformation M_s (intermediate γ_{tw}) such as the above-considered case of the Fe-Pd alloy, and (iii) the comparatively high-energy adaptive martensite (high γ_{tw}), which may form only during the nucleation stage to bypass the completely blocked nucleation of the normal martensite; the adaptive martensite immediately transforms into the normal martensite when the nucleation barrier is surmounted. In cases (ii) and (iii) the formation of the adaptive phase can be perceived as the premartensitic phenomenon.

As has been mentioned above, the crystal-lattice structure of the adaptive martensite is very sensitive to the applied stress. The other feature, predicted for the adaptive martensite structure, is the "incommensurate" position of its diffraction spots related to accommodation shuffling of crystal planes. This effect is caused by random faulting of the periodic distribution of shuffling planes, since such a faulting, like the formation of stacking faults in the fcc lattice, results in a shift of the diffraction spots from their regular positions. The value of the shift depends on the density of faults, and, thus, is determined by the crystal-lattice mismatch. It also depends on the diffraction indexes of the diffraction spots and, thus, the shift is different in different Brillouin zones. A true incommensurate phase can, however, be distinguished from a randomly faulted adaptive phase, since the positions of the diffraction spots of the former are the same in all Brillouin zones, while the positions of the latter are not.

Now let us consider a structural transition of the

second order. If the symmetry of the irreducible representation of the space group inducing the transformation is such that crystal-lattice parameters of the low-temperature phase are linear functions of the long-range order parameter, then the ratio $\gamma_{tw}/\mu\epsilon_0^2$ entering Eq. (1) tends to zero when temperature is close to the second-order transition. If the ratio is close to zero, then the adaptive phase should be formed. Therefore, the appearance of the adaptive phase just below the second-order transition should be expected. It should generate extra diffraction spots associated with regularly spaced accommodation faults with a period of the order of the correlation length. If there is a certain randomness in the fault distribution, then the position of the spots is incommensurate. To distinguish this structure from the real periodic incommensurate structure, the positions of the extra diffraction spots in different Brillouin zones should be investigated. The Fe-Pt alloys discussed in this paper are an example of the system where these phenomena can be observed. Similar phenomenon can be expected in the case when the transformation is a "soft" first-order transition. From this viewpoint a close look at the origin of some incommensurate phases observed near the second-order or first-order soft transition before the normal phase emerges would be useful.

ACKNOWLEDGMENTS

The authors are grateful to Professor K. Otsuka and Professor A. Roytburd for very useful discussions. A.G.K. and S.S. gratefully acknowledge support from Division of Materials Science, U. S. Department of Energy under Grant No. DE-FG05-90ER45430. They also thank Brookhaven National Laboratory where most of this work was done. The work at Brookhaven was supported by the Division of Materials Science of the U.S. Department of Energy under Contract No. DE-AC02-76CH00016.

*Also at Brookhaven National Laboratory, Upton, NY 11973.

¹M. S. Wechsler, D. S. Lieberman, and T. A. Read, *Trans. Metall. Soc. AIME* **197**, 1503 (1953).

²J. C. Bowles and J. K. Mackenzie, *Acta Metall.* **2**, 129 (1954); **2**, 138 (1954); **2**, 224 (1954).

³A. G. Khachaturyan, *Zh. Eksp. Teor. Fiz.* **56**, 1037 (1969) [*Sov. Phys. JETP* **29**, 557 (1969)].

⁴A. L. Roytburd, *Fiz. Tverd. Tela (Leningrad)* **10**, 3619 (1968) [*Sov. Phys. Solid State* **10**, 2870 (1969)].

⁵A. G. Khachaturyan, *Theory of Structural Transformations in Solids* (Wiley, New York, 1983).

⁶L. D. Landau and E. M. Lifshitz, *Phys. Zs. UdSSR* **8**, 153 (1935).

⁷S. Hendricks and E. Teller, *Chem. Phys.* **10**, 147 (1969).

⁸M. S. Paterson, *J. Appl. Phys.* **23**, 865 (1952).

⁹K. Enami, S. Nenno, and K. Shimizu, *Trans. Jpn. Instrum. Metals* **14**, 161 (1973).

¹⁰S. Rosen and J. A. Goebel, *Metall. Trans. AIME* **242**, 722 (1968).

¹¹V. V. Litvinov, A. A. Arhangel'skaya, and V. V. Poleva, *Fiz.*

Met. Metalloved. **38**, 383 (1974).

¹²K. Enami, S. Nenno, and K. Shimizu, *Trans. Jpn. Inst. Met.* **14**, 161 (1972).

¹³S. M. Shapiro, B. X. Yang, G. Shirane, Y. Noda, and L. E. Tanner, *Phys. Rev. Lett.* **62**, 1298 (1989).

¹⁴V. V. Martynov, K. Enami, L. G. Khandros, S. Nenno, and A. V. Tkachenko, *Phys. Met. Metallogr. (U.S.S.R.)* **55**, 136 (1983).

¹⁵V. V. Martynov, K. Enami, L. G. Khandros, A. V. Tkachenko, and S. Nenno, *Scr. Metall.* **17**, 1167 (1983).

¹⁶B. E. Warren, *X-Ray Diffraction* (Addison-Wesley, Reading, MA, 1969).

¹⁷R. Berliner, O. Fagan, H. G. Smith, and R. L. Hitterman, *Phys. Rev. B* **40**, 12086 (1989).

¹⁸Y. Noda, S. M. Shapiro, G. Shirane, Y. Yamada, and L. E. Tanner, *Phys. Rev. B* **42**, 10397 (1990).

¹⁹H. Warlimont and L. Delaey, *Martensitic Transformations in Cu-Ag- and Au-Based Alloys*, Vol. 18 of *Progress in Materials Science*, edited by B. Chalmers, J. W. Christian, and T. B. Massalski (Pergamon, Oxford, 1974).

²⁰M. Matsui, H. Yamada, and K. Adachi, *J. Phys. Soc. Jpn.* **48**,

- 2161 (1980).
- ²¹M. Sugiyama, K. Ohshima, and F. F. Fujita, *Trans. Jpn. Ints. Met.* **27**, 719 (1986).
- ²²H. Seto, Y. Noda, and Y. Yamada, *J. Phys. Soc. Jpn.* **59**, 965 (1990).
- ²³T. Maki and C. M. Wayman, *Proceedings of the International Symposium on New Aspects of the Martensitic Transformation, Kobe, Japan, 1976*, (Japan Institute of Physics, Sendai, 1977), p. 69.
- ²⁴L. Vinnikov, I. Georgieva, and L. Maystrenko, *Metallofizika*, **55**, 24 (1974).